Molecular Dynamics Simulation and Binding Studies of β-Sitosterol with Human Serum Albumin and Its Biological Relevance

ARTICLE *in* THE JOURNAL OF PHYSICAL CHEMISTRY B · JULY 2010

Impact Factor: 3.3 · DOI: 10.1021/jp102730p · Source: PubMed

5 AUTHORS, INCLUDING:

Babu Sudhamalla
University of Pittsburgh
13 PUBLICATIONS **241** CITATIONS
SEE PROFILE

Mahesh Gokara
University of Hyderabad
9 PUBLICATIONS **256** CITATIONS
SEE PROFILE

Navjeet Ahalawat
Indian Institute of Science Education and …
6 PUBLICATIONS **99** CITATIONS
SEE PROFILE

Rajagopal Subramanyam
University of Hyderabad
58 PUBLICATIONS **923** CITATIONS
SEE PROFILE

Molecular Dynamics Simulation and Binding Studies of β-Sitosterol with Human Serum Albumin and Its Biological Relevance

Babu Sudhamalla,[†,§] Mahesh Gokara,[†] Navjeet Ahalawat,[†,§] Damu G. Amooru,[‡] and Rajagopal Subramanyam*[,†]

Department of Biochemistry, School of Life Sciences, University of Hyderabad, 500046, India, Department of Biotechnology, School of Life Sciences, University of Hyderabad, 500046, India, and Department of Chemistry, Yogi Vemana University, Kadapa, Andhrapradesh, 516003, India

Received: March 26, 2010; Revised Manuscript Received: May 24, 2010

β-Sitosterol is a naturally occurring phytosterol that is widely used to cure atherosclerosis, diabetes, cancer, and inflammation and is also an antioxidant. Here, we studied the interaction of β-sitosterol, isolated from the aerial roots of *Ficus bengalensis,* with human serum albumin (HSA) at physiological pH 7.2 by using fluorescence, circular dichroism (CD), molecular docking, and molecular dynamics simulation methods. The experimental results show that the intrinsic fluorescence of HSA is quenched by addition of β-sitosterol through a static quenching mechanism. The binding constant of the compound to HSA, calculated from fluorescence data, was found to be $K_{\beta\text{-sitosterol}} = 4.6 \pm 0.01 \times 10^3\ M^{-1}$, which corresponds to −5.0 kcal M^{-1} of free energy. Upon binding of β-sitosterol to HSA, the protein secondary structure was partially unfolded. Specifically, the molecular dynamics study makes an important contribution to understanding the effect of the binding of β-sitosterol on conformational changes of HSA and the stability of a protein−drug complex system in aqueous solution. Molecular docking studies revealed that the β-sitosterol can bind in the large hydrophobic cavity of subdomain IIA, mainly by the hydrophobic interaction but also by hydrogen bond interactions between the hydroxyl (OH) group of carbon-3 of β-sitosterol to Arg(257), Ser(287), and Ala(261) of HSA, with hydrogen bond distances of 1.9, 2.4, and 2.2 Å, respectively.

I. Introduction

β-Sitosterol is a phytosterol or plant sterol compound, found in a variety of fruits, vegetables, and seeds, that has a variety of pharmacological properties.[1] The molecular mass is 414.7 Da and its molecular formula is $C_{29}H_{50}O$ (see Figure 1, insert) and similar to the cholesterol structure. It blocks cholesterol absorption resulting in lower serum cholesterol levels,[2] and also prevents the oxidation of LDL cholesterol, thereby reducing the risk of atherosclerosis.[3,4] It has been used to treat prostate problems such as benign prostatic hypertrophy and helps to increase urine flow;[5–7] thus, it may reduce the growth of the prostate gland, as well as inhibiting colon cancer cells and altering membrane lipids.[8,9] Other important roles include controlling the blood sugar and insulin levels in type II diabetes,[10] and helping to prevent temporary immune weakness that typically occurs during recovery from endurance exercise. It also is an active anti-inflammatory[11] antioxidant able to reduce DNA damage, reduce the level of free radicals in cells, stimulate lymphocyte production, and increase the level of typical antioxidant enzymes.[12–14]

Knowledge of interaction mechanisms between drugs and plasma proteins is of crucial importance for us to understand the pharmacodynamics and pharmacokinetics of a drug. Drug binding influences the distribution, excretion, metabolism, and interaction with the target tissues. Human serum albumin (HSA) is an important plasma protein responsible for the binding and transport of many endogenous and exogenous substances including hormones, fatty acids, and foreign molecules such as drugs.[15–28] HSA is synthesized and secreted from liver cells. It is the most abundant protein in plasma, and is both a transport and a depot protein. Also, it is a vital protein in maintaining normal osmolarity in plasma as well as in interstitial fluid. Structurally, HSA is a nonglycosylated single-chained polypeptide having a 67 kDa mass, which organizes to form a heart-shaped protein with approximately 67% α-helical content.[16–20] HSA is a widely studied protein because its primary structure is well-known and its tertiary structure has been determined by X-ray crystallography.[16]

HSA, a 585 amino acid residue protein, is monomeric but contains three structurally similar α-helical domains, namely, I (residues 1−195), II (196−383), and III (384−585), each consisting of two subdomains (A and B), and the overall structure is stabilized by 17 disulfide bridges.[16–20] An electron density corresponding to residues 1−4 and residues 583−585 of the HSA molecule is not clearly observed, probably because of conformational flexibility at both termini.[29] Aromatic and heterocyclic ligands have been found to bind within two hydrophobic pockets in subdomains IIA and IIIA, which are designated as site I and site II, respectively.[16–20] Site I is dominated by strong hydrophobic interaction with most neutral, bulky, heterocyclic compounds, while site II binds mainly by dipole−dipole, van der Waals, and/or hydrogen-bonding interactions with many aromatic carboxylic acids. HSA contains a single intrinsic tryptophan residue at position 214 in domain IIA, and its fluorescence is sensitive to the ligands bonded nearby.[30,31] Therefore, it is often used as a probe to investigate the binding properties of drugs with HSA. Recently, our group reported that the pentacyclic triterpenoid betulinic acid and

* Corresponding author. Address: Department of Biochemistry, School of Life Sciences, University of Hyderabad, 500 046 India. Tel: +91-40-23134572. Fax: +91-40-23010120. E-mail: srgsl@uohyd.ernet.in.
† Department of Biochemistry, University of Hyderabad.
‡ Department of Chemistry, Yogi Vemana University.
§ Department of Biotechnology, University of Hyderabad.

10.1021/jp102730p
Published on Web 06/21/2010

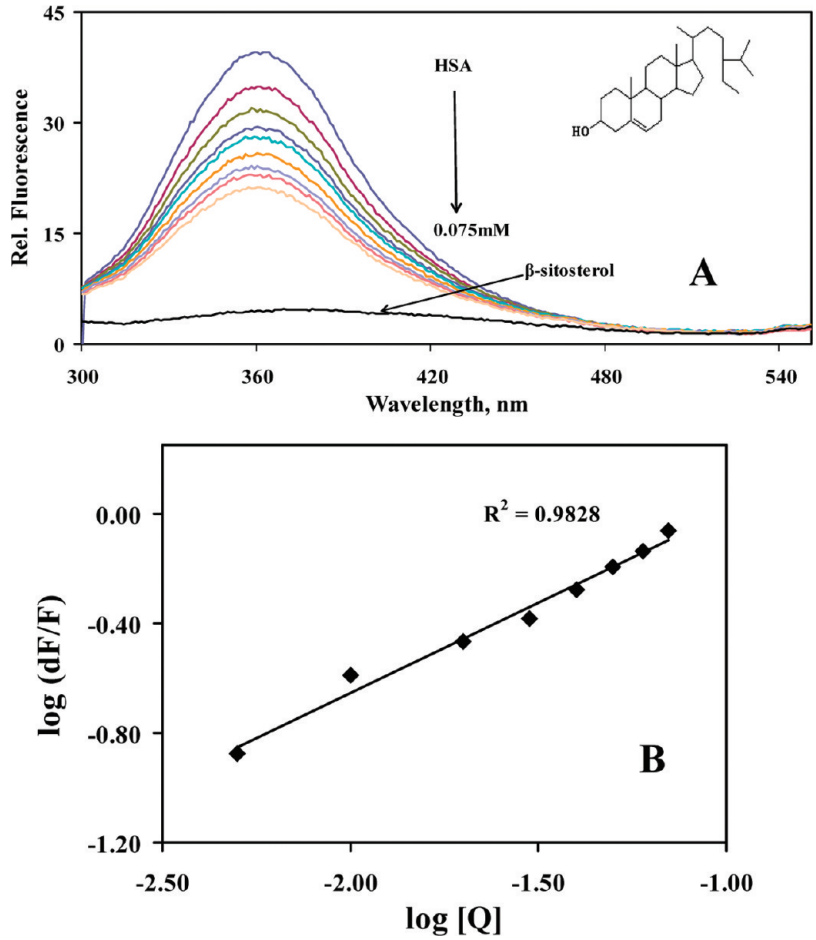

Figure 1. Fluorescence emission spectra of HSA−β-sitosterol in 0.1 M phosphate buffer pH 7.2, λ_{ex} = 285 nm, temperature =25 ± 1 °C. (A) Free HSA (0.025 mM) and free HSA with different concentrations of β-sitosterol (0.005, 0.01, 0.02, 0.03, 0.04, 0.05, 0.06, and 0.075 mM). (B) Plot of log (d*F*/*F*) against log [*Q*]. λ_{ex} = 285 nm, λ_{em} = 362 nm. For further details, see Materials and Methods.

feruloyl-maslinic acid, natural products isolated from *Tephrosia calophylla* and *Tetracera asiatica*, strongly bind to HSA.[32,33] Also, other natural compounds reported from our lab that trimethoxy flavone and coumaroyltyramine isolated from *Andrographis viscosula* and *Physalis minima* shows reasonable binding to HSA at IIIA and IIA domains, respectively.[34,35]

Considering the fact that β-sitosterol products play a major role in many biological processes,[1] it is important to understand the interactions of this compound with a major carrier protein such as HSA. In the present work, we isolated and identified β-sitosterol from the aerial roots of *Ficus bengalensis* and studied the interaction of HSA with β-sitosterol under physiological pH, using fluorescence, electrospray ionization (ESI) mass spectrometry, circular dichroism (CD), molecular dynamics (MD) simulations, and molecular docking studies.

II. Materials and Methods

A. Extraction, Isolation, and Identification. Herbal preparations of *F. bengalensis* Linn (Moraceae) (collected in South India), have been considered effective and safe ethnomedicines to treat pains, bruises, rheumatism, lumbago, sores, and ulcers in the Indian traditional system of medicine. The hanging roots of *F. bengalensis* have been reported to be antidiabetic, antidiarrheal, antitumor, and antibacterial agents.[36–38] Fresh aerial roots of *F. bengalensis* (23.1 kg) were shade-dried, powdered, and extracted with hot MeOH (20 L × 5) and concentrated to give a dark brown syrup (230 g), which was partitioned between H_2O and $CHCl_3$, and then *n*-BuOH. This resulted in $CHCl_3$, *n*-BuOH, and H_2O soluble portions after evaporating the solvent. The $CHCl_3$ solubles (48 g) were chromatographed on silica gel using step gradients of *n*-hexane and EtOAc (8:2, 7:3, and 1:1) to afford five fractions. Fraction 1 was rechromatographed on silica gel using *n*-hexane−EtOAc mixtures (9:1, 5:1, 3:1, and 1:1) as eluents to obtain β-sitosterol (126 mg) along with several other steroids and phenanthroindolizidine alkaloids. β-Sitosterol was identified by comparison of its spectroscopic data (UV, IR, NMR, mass spectrometry) with the values for an authentic sample.

B. Preparation of Stock Solutions. Pure fat-free HSA (a kind gift from Virchow Biotech Pvt Ltd., Hyderabad) was dissolved at a concentration of 1.5 mM in physiological aqueous solution (0.1 M phosphate buffer pH 7.2). β-Sitosterol (obtained from Dr. A.G. Damu, Yogi Vemana University, Kadapa, India) was prepared (2 mM) in 20:80% ethanol/water mixture. It should be noted that 20% ethanol does not affect the absorption of HSA and its structure.[32] β-Sitosterol was pure and has a molecular mass of 414.7 Da, which was demonstrated by matrix-assisted laser desorption ionization time-of-flight (MALDI-TOF) (data not shown). All other chemicals were purchased from Sigma Aldrich.

We suspended the aqueous HSA in 0.1 M phosphate buffer at different pH values to find the optimum physiological pH by measuring its absorption. The maximum absorption was observed at pH 7.2, thus, for determining the remaining parameters, we used 0.1 M phosphate buffer, pH 7.2, as a physiological buffer. We also optimized the time of β-sitosterol binding to

HSA by fluorescence emission and CD spectroscopy, and we found that 30 min is the optimum binding time. Thus, we have fixed the incubation of β-sitosterol with HSA for 30 min in all parameters.

C. Fluorescence Spectroscopy. The fluorescence emission spectra were recorded on a FluoroMax-3, Jobin-Yvon instrument from 300 to 500 nm, with an excitation wavelength of 285 nm. The final concentrations of the β-sitosterol were 0.005, 0.01, 0.02, 0.03, 0.04, 0.05, 0.06, and 0.075 mM with 0.1 M phosphate buffer pH (7.2), and the protein concentration was fixed 0.025 mM. The binding constant was calculated using the maximum fluorescence value at 362 nm. Three independent experiments were performed, and identical spectra were obtained.

D. ESI Mass Spectrometry (Micro TOF-Q). Positive ion mode mass spectra were recorded on a Micro TOF-Q mass spectrometer (Bruker Daltonics, Bremen, Germany) equipped with an ESI source. Free HSA and HSA$-\beta$-sitosterol were prepared in 5 mM ammonium acetate (pH 7.2) mixed with 20% acetonitrile, and introduced into the mass spectrometer source with a syringe pump (KD Scientifics Inc., Hilliston, MA) at 3 μL/min. Electrospray was performed by setting the spray voltage at 4.5 kV and the capillary temperature at 200 °C. The nebulizer gas was prepurified nitrogen (99.999%) with a flow rate of 4 L/min, and argon was used as the collision gas. The TOF pressure was maintained at less than 4×10^{-5} Pa. Scanning was performed over an *m*/*z* range from 50 to 3000 with a collision energy of 10 eV and data were averaged for 2 min and then smoothed using the Gaussian algorithm in the Bruker Data Analysis 3.4 software program. The instrument was calibrated using ES Tuning Mix (Agilent Technologies, part No. G2421-60001), injected by a divert valve just before sample application.

E. CD Spectroscopy. CD spectra of HSA and HSA$-\beta$-sitosterol were recorded with a Jasco J-810 spectropolarimeter using a quartz cell with a path length of 0.02 cm. Three scans were accumulated at a scan speed of 100 nm min^{-1}, with data being collected at every nm from 190 to 300 nm. For CD studies, the final concentration of HSA was 0.025 mM and the concentrations of β-sitosterol were 0.01, 0.025, 0.05, and 0.075 mM. Secondary structure determination was done using CDNN 2.1 software.

F. Molecular Modeling and Docking. The advanced molecular docking program GOLD (Genetic Optimization for Ligand Docking), which uses a powerful genetic algorithm (GA) method for conformational search and docking programs, was employed to generate an ensemble of docked conformations.[39–41]

Preparation of the Protein and the Ligand. The known crystal structure of HSA (PDB Id: 1AO6) was obtained from the Brookhaven Protein Data Bank. From the two-dimensional (2D) structure the three-dimensional (3D) structure of β-sitosterol was built, and its geometry was optimized through discover3 in the InsightII/Builder program. Water molecules and ions were removed (including ordered water molecules), and hydrogen atoms added to functional groups with the appropriate geometry within the protein, which was ionized as required at physiological pH. The structure of HSA was protonated in InsightII (www.accelrys.com). A GA was implemented in GOLDv3.2, which was applied to calculate the possible conformations of the drug that binds to the protein. The GA parameters used are as follows: active site radius - 30; population size - 100; number of islands - 5; niche size - 2; selection pressure - 1.1; migrate - 10; number of operators - 100 000; mutate - 95; crossover - 95. The default speed selection was used to avoid a potential reduction in docking accuracy. Fifty GA runs with default parameter settings were performed without early termination. To estimate the protein−ligand complexes (scoring function) GOLD score was employed.[40]

During the docking process, a maximum of 10 different conformations were considered for the drug. Among these, the best and the most energetically favorable conformations with fairly similar GOLD fitness scores of each ligand were selected. The conformer with the lowest binding free energy with the highest fitness score was used for further analysis.[40]

AutoDock Analysis. AutoDock generated the different ligand conformers using a Lamarkian GA, a GA implementation with an adaptive local method search.[42] The simulations started with a predefined number of generation cycles, composed of mapping and fitness evaluation, selection, crossover, mutation and elitist selection steps, and continued with a local search, followed by the scoring of the generated conformers. The energy-based AutoDock scoring function includes terms accounting for short-range van der Waals and electrostatic interactions, loss of entropy upon ligand binding, hydrogen bonding, and solvation. The protein and the ligand input structures, prepared as described above, were transformed into the corresponding pdbq format files (containing atom coordinates, partial charges, and solvation parameters), with the mol2- to pdbqs and AutoTors programs, respectively. To recognize the binding sites in HSA, blind docking was carried out, the grid size set to 126, 126, and 126 along the *X*, *Y*, and *Z* axes with 0.597 Å grid spacing. The center of the grid set to 29.53, 31.83, and 23.49 Å. The AutoDocking parameters used were GA population size: 150 and maximum number of energy evolutions: 250 000. During docking, a maximum number of 10 conformers was considered, and the root-mean-square (rms) cluster tolerance was set to 2.0 Å. One of the lowest energy conformations was used for further analysis (Table 1), which matches the experimental values (see sections III.B and III.C).

G. MD Simulations. A 6000 ps MD simulation of the complex was carried out with the GROMACS4.0[43,44] package using the GROMOS96 43a1 force field.[45,46] The initial conformation was taken from one of the lowest binding energy docking conformation (Table 1). The topology parameters of HSA were created by using the Gromacs program. The topology parameters of β-sitosterol were built by the Dundee PRODRG2.5 server (beta).[47] Then the complex was immersed in a cubic box ($7.335 \times 6.135 \times 8.119$ nm^3) of extended simple point charge (SPC) water molecules.[48] The solvated system was neutralized by adding sodium ions in the simulation, and the entire system was composed of 5843 atoms of HSA, one β-sitosterol, 15 Na^+ counterions and 69491 solvent atoms. To release conflicting contacts, energy minimization was performed using the steepest descent method of 1000 steps, followed by the conjugate gradient method for 1000 steps. MD simulation studies consist of equilibration and production phases. In the first stage of equilibration, the solute (protein, counterion, and β-sitosterol) was fixed and the position-restrained dynamics simulation of the system, in which the atom positions of HSA were restrained at 300 K for 30 ps. Finally, the full system was subjected to 6000 ps MD at 300 K temperature and 1 bar pressure. The periodic boundary condition was used and the motion equations were integrated by applying the leaf-frog algorithm with a time step of 2 fs. The atom coordinates were recorded every 0.5 ps during the simulation for latter analysis. The MD simulation and results analysis were performed on the OSCAR Linux cluster with 16 node (dual xeon processor) at the CMSD facility, University of Hyderabad, India.

TABLE 1: Docking Summary of HSA with β-Sitosterol by the AutoDock Program Generating Different Ligand Conformers Using a Lamarkian GA[a]

rank	run	binding energy [kcal M^{-1}]	K_i	K_a [M^{-1}]	cluster rmsd	ligand efficiency	reference rmsd
1	7	−9.37	134.34 nM	7.45×10^6	0.00	−0.31	49.76
2	1	−9.26	162.73 nM	6.14×10^6	0.00	−0.31	49.58
3	2	−8.63	471.53 nM	2.12×10^6	0.00	−0.29	47.29
3	9	−8.28	847.96 nM	1.18×10^6	1.68	−0.28	47.00
4	8	−8.61	489.41 nM	2.04×10^6	0.00	−0.29	47.12
5	6	−7.54	2.98 μM	3.35×10^5	0.00	−0.25	45.09
6	10	−7.41	3.67 μM	2.72×10^5	0.00	−0.25	44.98
7	5	−7.33	4.27 μM	2.34×10^5	0.00	−0.24	45.70
8	3	−5.89	48.19 μM	2.07×10^4	0.00	−0.2	24.80
9	**4**	**−5.42**	**106.85 μM**	9.36×10^3	**0.00**	**−0.18**	**27.84**

[a] The bold font indicates one of the lowest free energy conformations, which matches Section III.B and C, and which is considered to be the most stable model.

III. Results and Discussion

A. Fluorescence Quenching of HSA in the Presence of β-Sitosterol. Figure 1A depicts the room-temperature fluorescence emission spectra of HSA in the presence of different concentrations of β-sitosterol with physiological phosphate buffer, pH 7.2. The typical emission peak was observed at 362 nm,[32,33] and the excitation wavelength was 285 nm. Upon incubation of different concentrations (0.005−0.075 mM) of β-sitosterol with HSA, the maximum fluorescence peak intensity was reduced without any peak shift. Thus it indicated that HSA−β-sitosterol complexes were formed. Fluorescence quenching is the decrease of the quantum yield of fluorescence from a fluorophore induced by a variety of molecular interactions with a quencher molecule. In general, the fluorescence of HSA comes from tryptophan, tyrosine, and phenylalanine residues. The intrinsic fluorescence of HSA is almost entirely due to tryptophan because phenylalanine has a very low quantum yield, and the fluorescence of tyrosine is almost totally quenched if it is ionized or near an amino group, a carboxyl group, or a tryptophan. This viewpoint was well supported by the experimental observations of Sulkowska.[49] The change of intrinsic fluorescence intensity of HSA was due to tryptophan residue when small molecules bound to HSA.

B. Evaluation of the Binding Constant and Binding Site. Fluorescence emission spectroscopy was used to quantify the binding constant of β-sitosterol to HSA. β-Sitosterol quenches the strong fluorescence emission band at 362 nm upon binding to HSA. Our results show that the intensity of HSA fluorescence decreases upon increasing the drug concentration (0.005 to 0.075 mM) with a fixed concentration of HSA (0.025 mM) (Figure 1). Similar fluorescence results were reported for the interaction of different ligand molecules with HSA.[21−28] Also, we have reported recently that natural compounds such as trimethoxy flavone and coumaroyltyramine quenched the emission fluorescence.[34,35] Thus, the decrease in fluorescence indicates that the β-sitosterol binding to HSA causes microenvironment changes in HSA due to the formation of HSA−β-sitosterol complexes. For static quenching, the binding constant (K_s) and the number of binding sites (n) can be derived from the following equation.[50]

$$\log(dF/F) = \log K_S + n \log[Q] \quad (1)$$

Where n is the number of ligands binding to the protein, K is the binding constant, and $[Q]$ is the drug concentration. The dF is $F_0 - F$, where F_0 is the initial fluorescence of free HSA and F is fluorescence with different concentrations of β-sitosterol. The linearity in the plot of log (dF/F) against log(Q) confirms a one-to-one interaction between β-sitosterol and HSA (see Figure 1B). From the slope of the plot, the binding constant of β-sitosterol to HSA was calculated to be $4.6 \pm 0.01 \times 10^3$ M^{-1}. We have also calculated the binding constant by using a different computation technique (see below), which shows K is 9.36×10^3 M^{-1}, thus this result was in reasonable agreement with the experimental data. As a reference, natural compound bindings similar to HSA were published recently from our group on betulinic acid, feruloyl masalinic acid, trimethoxy flavone, and coumaroyltyramine, and their binding constants were $K_{BA} = 1.685 \pm 0.01 \times 10^6$ M^{-1}, $K_{FMA} = 1.42 \pm 0.01 \times 10^8$ M^{-1}, $K_{TMF} = 1.0 \pm 0.01 \times 10^3$ M^{-1}, and $K_{CT} = 4.5 \pm 0.01 \times 10^5$ M^{-1}.[32−35] Other molecules like flavanoids exhibit binding constants in the range of $1-15 \times 10^4$ M^{-1}.[51] Small molecules such as resveratrol hexadecanoate and resveratrol gave binding constants of 6.70×10^6 M^{-1} and 1.64×10^5 M^{-1}, respectively.[52] Naturally occurring compounds such as resveratrol, genistein, and curcumin bind bovine serum albumin with constants of 2.52×10^4 M^{-1}, 1.26×10^4 M^{-1}, and 3.33×10^4 M^{-1}, respectively.[53]

C. Free Energy Calculations. Generally, there are four types of noncovalent interaction in ligand binding to proteins. These are hydrogen bonds, van der Waals forces, hydrophobic bonds, and electrostatic interactions. The thermodynamic parameters of the binding reaction are the main evidence for confirming the forces involved. The standard free energy is calculated according to eq 2.

$$\Delta G^0 = -RT \ln K \quad (2)$$

Where ΔG is free energy, K is the binding constant at the corresponding temperature, which can be obtained from fluorescence data, and R is the gas constant. Thus, the free energy change is −5.0 kcal M^{-1} at 25 °C. We have also calculated the free energy (−5.42 kcal/mol) from computation modeling (Table 1), and it is in agreement with the experimental data. Here the lower free energy value is mainly the hydrophobic interactions of β-sitosterol binding to HSA. Hydrogen bond interactions also could be present. These results were fully supported by computational calculations (see section III.F). Similar results reported by Li et al[54] indicated that 8-acetyl-7-hydroxycoumarin interacts with HSA through hydrophobic and hydrogen bonding. In addition, similar types of interactions such as hydrophobic and hydrogen bonding were observed with our recent studies of natural compounds, feruloyl maslinic acid, trimethoxy flavone, and coumaroyltyramine with HSA.[34,35]

D. Micro TOF-Q Analysis. The complexation of β-sitosterol with HSA at micromolar levels was demonstrated using a micro

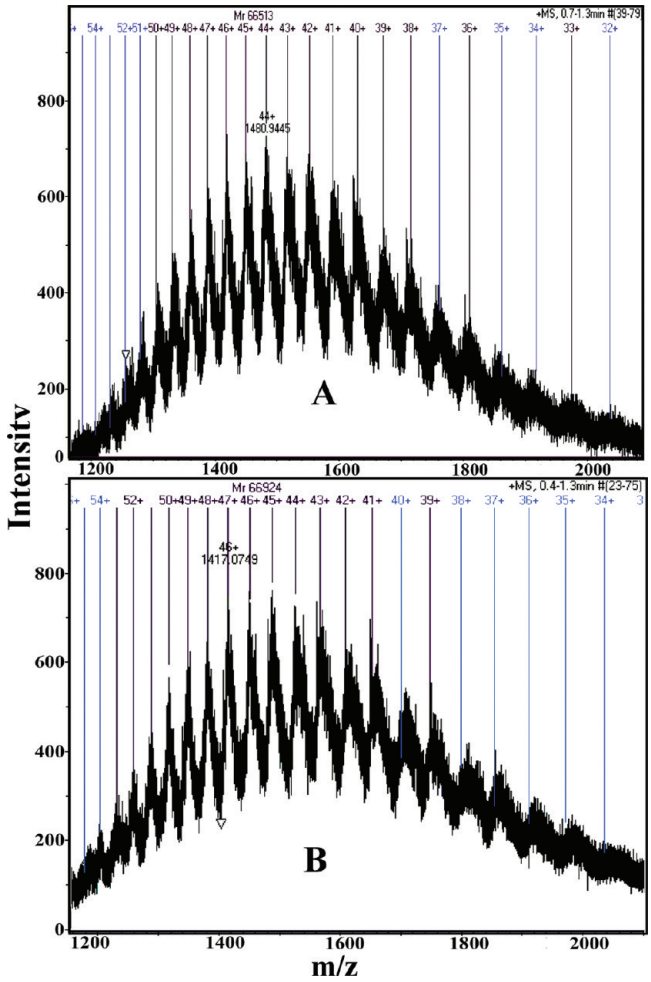

Figure 2. (A) Micro TOF-Q mass spectra of free HSA. (B) HSA along with β-sitosterol. The concentration of free HSA and β-sitosterol were 0.15 μM and 0.5 μM, respectively. *m*/*z*, where *m* is mass and *z* is the charge of the molecule. For further details, see Materials and Methods.

TOF-Q mass spectrometer. Figure 2A,B depicts the mass spectra of free HSA and HSA complexes. The numbers on the dark vertical lines indicate the matched charge states of HSA or HSA+ β-sitosterol complexes. Deconvolution of the multiply charged states resulted in the mass determinations for HSA and the HSA-β-sitosterol complex. When β-sitosterol was bound to free HSA, the molecular mass increased from 66513 to 66924 Da, which suggests that β-sitosterol did indeed bind to HSA. Since the molecular weight of β-sitosterol is 414.7 Da, the additional mass of ~411 Da indicated that one molecule of β-sitosterol was bound to HSA. This result is in agreement with fluorescence data and reveals that the interaction of β-sitosterol with HSA is 1:1. Recently, our group reported that natural compounds such as betulinic acid and trimethoxy flavone bound to HSA were 1:1, which was determined by fluorescence emission as well mass spectrometry.[34,35]

E. CD Spectroscopy Studies. CD spectroscopy is one of the finest methods for identification of the conformational changes of proteins whose secondary structure may vary in accordance with their bound state. The CD spectra of HSA exhibit two negative bands in the ultraviolet region, at 208 and 218 nm. When various concentrations of β-sitosterol were added to free HSA and incubated for 30 min, the intensities at 208 and 218 nm decreased in a concentration-dependent manner. This clearly demonstrates considerable changes in the protein

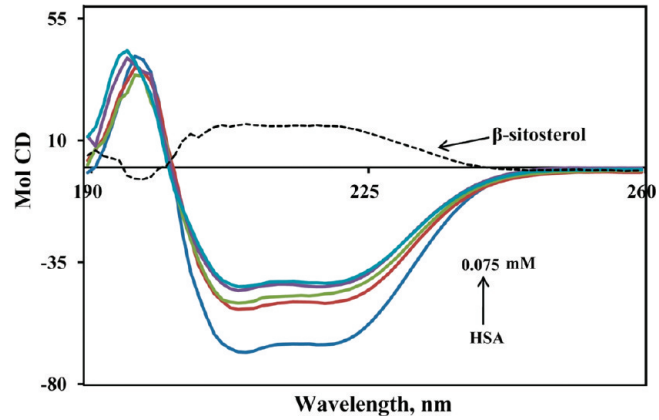

Figure 3. CD spectra of free HSA and its β-sitosterol analogue complexes in aqueous solution with a protein concentration of 0.025 mM and β-sitosterol concentrations of 0.01, 0.025, 0.05, and 0.075 mM.

secondary structure. Specifically, it suggested the loss of helical stability, and may be the result of the formation of a complex between HSA and the β-sitosterol. Secondary-structural elements were calculated by using the CDNN program. In free HSA, secondary structure consists of ~57.5% α-helix, ~24.6% β-sheets and ~17.9% random coils, which is in agreement with earlier reports.[23,32–35] The proportion of secondary structural elements undergoes marginal variation at low concentrations of β-sitosterol (see Figure 3, Table 2). However, with the addition of 0.05 and 0.075 mM of β-sitosterol, there was a significant change in protein conformation. At 0.075 mM concentration, the α-helical content decreased to ~38.20%, while the proportion of β-sheets and random coils increased to ~33% and ~28.8%, respectively (Table 2). These results indicate that the secondary structure of HSA became partially unfolded due to HSA−β-sitosterol complex formation. Secondary structural conformational changes occur as interior flexibility of the IIA domain of HSA due to binding of β-sitosterol. Consequently, we see the CD signal changes upon binding of β-sitosterol to HSA. Very recently, our group reported that *N-trans-p*-coumaroyltyramine, a natural compound bound to HSA, leads to conformational changes due to inherent flexibility at the IIA domain.[35] Similar results were observed upon binding of other ligands (pentacyclic triterpenoids derivatives of betulinic acid and feruloyl maslinic acid, trimethoxy flavone, coumaroyltyramine, flavonoids, quercetin, crocetin, dimethylcrocetin, safranal, retinol, retinoic acid, and resveratrol aliphatic acid) to HSA, thus indicating a major decrease of α-helices and an increase of β-sheets and random coils as well.[32–35,50–57] For a reference, polyamine analogues binding to HSA showed a change in protein secondary structure, major alterations with a reduction of α-helix from 55% (free protein) to 43%, and an increase of β-sheet from 17% (free protein) to 29−36% in the 333, BE-333, and BE-3333 complexes, indicating partial protein unfolding upon polyamine interaction.[56]

F. Molecular Docking Studies. Crystal structure analysis[15] has revealed that HSA consists of a single polypeptide chain of 585 amino acid residues and comprises three structurally homologous domains (I−III): I (residues 1−195), II (196−383), and III (384−585) that assemble to form a heart-shaped molecule. The principal regions of ligand binding sites of HSA are located in hydrophobic cavities in subdomains IIA and IIIA, which correspond to sites I and site II, respectively. The sole tryptophan residue (Trp-214) of HSA is in subdomain IIA. There is a large hydrophobic cavity present in subdomain IIA, and many drugs can bind in this location.

TABLE 2: Secondary Structural Analysis of the Free HSA and Its Interaction with β-Sitosterol[a]

	free HSA (mM)	HSA+0.01 (mM)	HSA+0.025 (mM)	HSA+0.05 (mM)	HSA+0.075 (mM)
α-helix (%)	57.5 ± 2.5	49.7 ± 2.5	47.6 ± 4.5	42.6 ± 2.5	38.2 ± 3.0
antiparallel (%)	6.8 ± 0.4	5.1 ± 0.4	5.4 ± 0.4	6.8 ± 0.4	7.4 ± 0.5
parallel (%)	4.8 ± 0.3	5.2 ± 0.34	5.6 ± 0.36	6.9 ± 0.45	7.3 ± 0.47
β-turn (%)	13 ± 0.74	14.75 ± 1.0	15.7 ± 0.84	16.5 ± 0.94	18.3 ± 1.04
random coil (%)	17.9 ± 1.0	25.25 ± 1.5	25.7 ± 1.5	27.2 ± 1.5	28.8 ± 1.7

[a] On the basis of Figure 3, the data was analyzed by web-based software CDNN 2.1.

In this study, the GOLD v3.2, AutoDock programs were chosen to examine the binding mode of β-sitosterol at the active site of HSA. The best score ranked results are shown in Table 1. The docking results showed that β-sitosterol binds within the binding pocket of subdomain IIA. The inside wall of the pocket of subdomain IIA is formed by hydrophobic side chains, whereas the entrance of the pocket is surrounded by positively charged residues, i.e., Arg257, Arg222, Lys199, His242, Arg218, and Lys195. It can be seen that the β-sitosterol molecule was situated within the subdomain IIA hydrophobic cavity (see

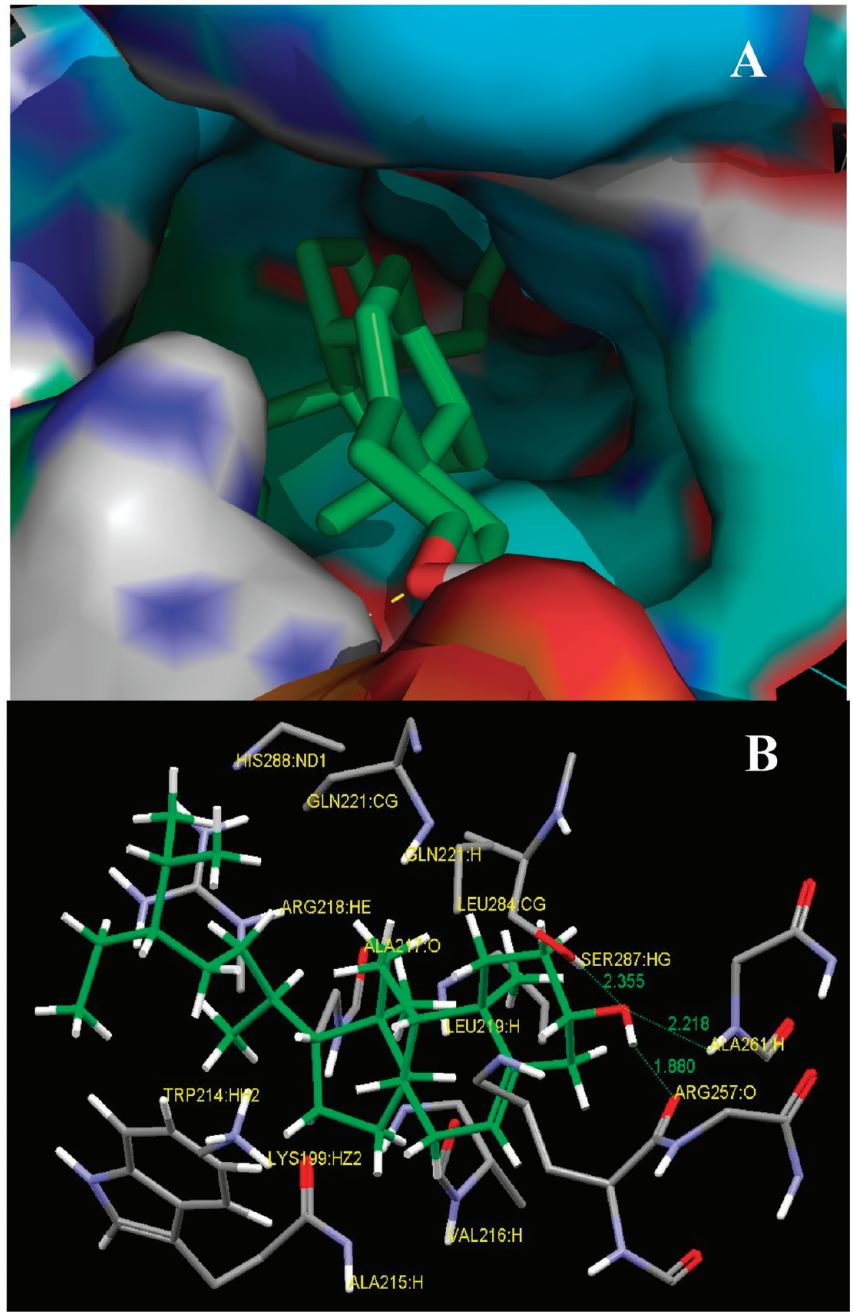

Figure 4. (A) β-Sitosterol docked in the binding pocket of HSA using GOLD v3.2. β-Sitosterol, depicted in a stick model (light green), and HSA, represented in solid (better) with a ray model. The image was made using Pymol (pymol.sourceforge.net). (B) Stereoview of the docking poses of the HSA−β-sitosterol complex (prepared by using a SILVER v1.1.1 visualizer). β-Sitosterol is rendered as capped sticks, and the residues are rendered as an ellipsoid model. Three H-bonds (as highlighted by the dashed lines in green color) formed between β-sitosterol and HSA.

Figure 4A). The β-sitosterol molecule moiety was located within the binding pocket, and several cyclohexyl groups of β-sitosterol were adjacent to Arg (218), Trp (214), Lys (199), and Leu (219) residues and so forth of the subdomain IIA of HSA (site 1). Thus, we can conclude that the interaction of β-sitosterol with HSA is a mainly hydrophobic, which is in perfect agreement with the thermodynamic results obtained from fluorescence emission (see section III.C). Furthermore, there were also a number of specific hydrogen bonds, because several polar residues in the proximity of the ligand play an important role in binding the β-sitosterol molecule via H-bonds. Hydrogen-bonding interactions were between the hydroxyl (OH) group of carbon-3 of β-sitosterol and Arg(257), Ser(287), and Ala(261) of HSA, with a hydrogen bond distances of 1.9, 2.4, and 2.2 Å, respectively (see Figure 4B). The results suggested that the formation of hydrogen bonds stabilize the β-sitosterol−HSA complexes. Similar results were observed for other ligand molecules bound to HSA.[47,50,51] The binding constant and free energy change ΔG^0 for the binding of β-sitosterol to HSA were 9.36×10^3 M^{-1} and −5.42 kcal M^{-1}, respectively. The above results closely matched the experimental data, which gave binding constant and free energy values of $4.6 \pm 0.01 \times 10^3$ M^{-1} and −5.0 kcal M^{-1}, respectively.

Therefore, the results of molecular docking indicate that the interaction between β-sitosterol and HSA are dominated by hydrophobic forces, which is agreement with the fluorescence data. It was important to note that the Trp-214 residue of HSA is in close proximity to the ligand molecule. This finding provides a good structural basis to explain the efficient fluorescence quenching of HSA emission in the presence of β-sitosterol. Our results have shown that β-sitosterol can interact with HSA at site I in subdomain IIA with hydrophobic and hydrogen bonding interactions, which is consistent with the previously published data on other ligand molecules.[35,52,54,58]

G. Analysis of the Dynamics Trajectories. To investigate the stability of the system (protein, ligand, water, ions, etc.) properties were examined by means of rms deviations (rmsd's) of protein and β-sitosterol with respect to the initial structure, rms fluctuations (rmsf's) and the radius of gyration (R_g) of protein. In addition, the stability of system proved the credibility of the docking result (Figure 4), where our β-sitosterols bound to HSA at drug binding site I, which is the IIA subdomain, were used for MD simulations.

The rmsd values of atoms in unliganded HSA and HSA−β-sitosterol complexes were plotted from 0 to 6000 ps as shown in Figure 5. Analysis of the Figure 5 indicates that the rmsd of both systems reaches equilibration and oscillates around in average value after 3000 ps simulation time. The rmsd values of atoms in HSA and HSA−β-sitosterol complexes were calculated from a 3000−6000 ps trajectory, where the data points were fluctuated for HSA, 0.72 ± 0.036 nm and HSA−β-sitosterol, 0.85 ± 0.023 nm, respectively.

In the present MD study, we determined the radius of gyration (R_g) values of unliganded HSA and HSA−β-sitosterol complex as shown in Figure 6. In both systems, R_g values were stabilized at about 3500 ps, indicating that the MD simulation achieved equilibrium after 3500 ps. Initially, the R_g values of both unliganded HSA and HSA−β-sitosterol complex was 2.7 nm. The unliganded HSA and HSA−β-sitosterol were stabilized at 2.59 ± 0.03 and 2.40 ± 0.031 nm, respectively (Figure 6). The earlier report shows that the R_g value of HSA experimentally shown by neutron scattering in aqueous solution was 2.74 ± 0.035 nm indicated that our MD simulations is matching to the experimental values reported earlier.[59] The above results suggest

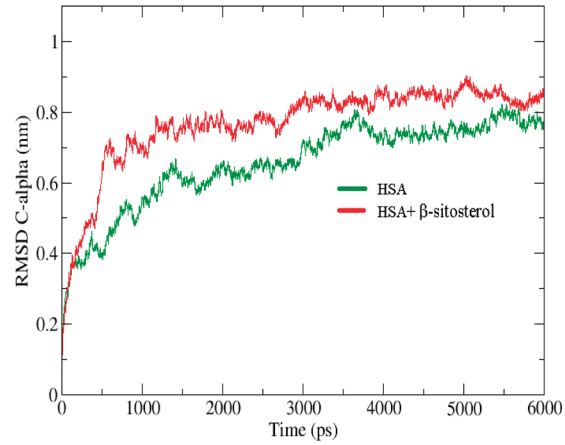

Figure 5. Time dependence of rmsd's. C_α rmsd values for unliganded HSA and HSA−β-sitosterol complex during 6000 ps MD simulation.

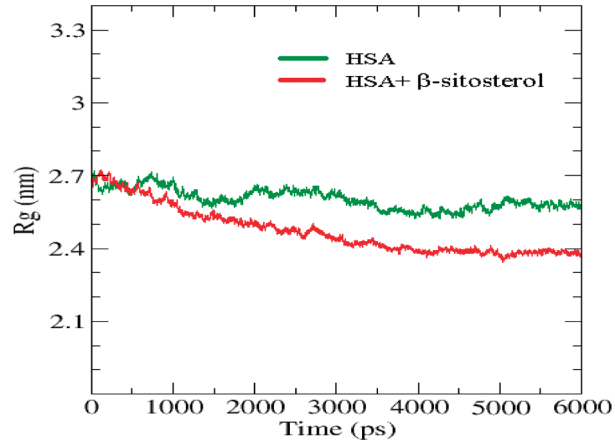

Figure 6. Time evolution of the radius of gyration (R_g) during 6000 ps of MD simulation of HSA and β-sitosterol.

that the radius of gyration value decreased upon β-sitosterol complexation with respect to free HSA. This clearly indicates that the β-sitosterol changes the microenvironment of HSA leads to the conformational changes in the HSA during MD simulation. This R_g value is strongly supported with the experimental CD data shown in Table 2. Upon β-sitosterol complexation with HSA, major HSA conformational changes were observed from CD analysis (Figure 3 and Table 2). Thus, our experimental data (CD) fully supports the MD simulation in which protein conformational changes occur during β-sitosterol binding to HSA. There are other reports supporting our results that protein conformational changes occurred during the MD simulation with albumin in the boundary lubrication process of an artificial joint,[60] binding fatty acids with HSA.[61] The conformational change of HSA depicts stabilization of HSA + β-sitosterol complexes in both CD and MD simulations. It is clearly shown in the MD simulation that, around 3500 ps, the HSA + β-sitosterol complexes were stabilized due to their conformational rearrangements. A similar report was shown in our group, that the orientation of the protein changes due to binding of coumaroyltyramine, [35] and similar reports showed the simulation data of different ligand molecules bound to HSA.[61,62]

Local protein mobility was analyzed by calculating the time-averaged rmsf values of free HSA and HSA−β-sitosterol complexes were plotted against residue numbers based on the 6000 ps trajectory data shown in Figure 7A. The profiles of atomic fluctuations were found to be very similar to those of

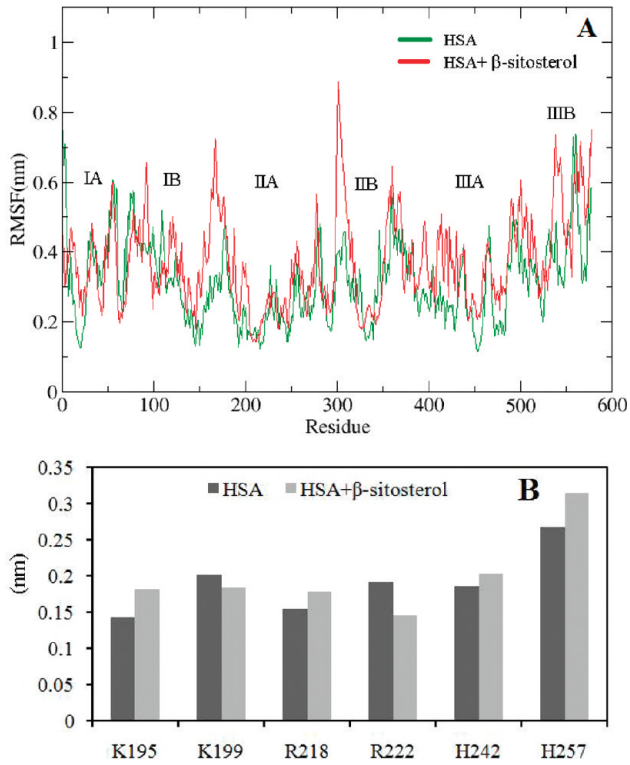

Figure 7. (A) The rmsf values of unliganded HSA and HSA−β-sitosterol complex were plotted against residue numbers. (B) The profile of atomic fluctuations of unliganded HSA and HSA−β-sitosterol complex (active site amino acid residues present in the IIA subdomain of HSA).

HSA and HSA-β-sitosterol complexes. Our result clearly indicates that subdomains IIB and IIIB of HSA have highest fluctuations, while subdomains IIA and IIIA present lower fluctuations. These results suggest that the structure of primary drug binding site I (IIA) remains rigid during simulation. The binding of β-sitosterol to HSA mainly affects the loop regions connecting the helices. Figure 7A shows that the highly fluctuating regions are three loops that connect helices: IB-h3 to IB-h4 (residues 170−173), IIA-h6 to IIB-h1 (residues 292−314) and IIIB-h3 to IIIB-h4 (residues 560−565). We investigated the profile of atomic fluctuations of residues at IIA subdomains K195, K199, R218, R222, H242, and R257 as shown in Figure 7B, which can affect the binding of β-sitosterol. In this site, the fluctuations are less compared with the other drug binding site (site II). This study provides evidence that HSA binding sites I (IIA subdomain) interact specifically with β-sitosterol through conformational adjustments of the protein structure, in conjunction with ligand conformational adaptation to these sites.

IV. Conclusion

Naturally occurring β-sitosterol was purified from the aerial roots of *F. bengalensis* and has potential value as a therapeutic agent to cure many diseases. Here we have tested this compound with HSA since it plays a major role in transporting the drug molecules to the target places. We have reported here that β-sitosterol binds to HSA with a binding constant of $K_{\beta\text{-sitosterol}} = 4.6 \pm 0.01 \times 10^3\ M^{-1}$ and free energy was −5.0 kcal M^{-1} at 25 °C. Upon complexation of β-sitosterol to free HSA, the protein secondary structure conformation is changed, so that α-helical content was reduced while β-sheets and random coils were increased. The molecular docking studies indicated that the β-sitosterol binds to the HSA at drug binding site I in the vicinity of Trp 214, which is in subdomain IIA, with hydrophobic and hydrogen bonding interactions. Specifically, the MD study makes an important contribution to understanding the effect of the binding of β-sitosterol on conformational changes of HSA and the stability of a protein−drug complex system in aqueous solution. MD simulation studies revealed that HSA and HSA−β-sitosterol complexes were stabilized around 3500 ps and also exhibited conformational change. The spectroscopic, molecular docking, and MD simulation study described herein is a promising approach for probing the interactions of plant medicines with relevant target proteins. Accurate measurements of sitosterol's albumin binding properties and knowledge of its binding site locations are important to prevent adverse drug reactions leading to life-threatening diseases such as heart disease, cancer, diabetes, and so forth. It is our hope that the results presented here provide new grounds for further investigations of the pharmaceutical potential of this plant molecule, and will be useful for monitoring its biological functions in vivo.

Acknowledgment. We thank Dr. N. Sreepadh, Virchow Biotech, Hyderabad, India, for a kind gift of pure HSA. The authors are grateful to Dr. Daniel C. Brune, Arizona State University, USA, for critical reading of this manuscript. We greatly acknowledge the School of Life Sciences, UOH-CREBB for providing the facility of micro-TOF-Q mass spectrometry at the University of Hyderabad. We thank CMSD and CIL, University of Hyderabad, for computational and CD facilities, respectively. This work was partially supported by DBT and DST, India.

References and Notes

(1) Mutai, C.; Bii, C.; Vagias, C.; Abatis, D.; Roussis, V. *J. Ethnopharmacol.* **2009**, *123*, 143.
(2) Cicero, A. F. G.; Fiorito, A.; Panourgia, M. P.; Sangiorgi, Z.; Gaddi, A. *J. Am. Diet. Assoc.* **2002**, *102*, 1807–1811.
(3) Vivancos, M.; Moreno, J. J. *Br. J. Nutr.* **2007**, *99*, 1199–1207.
(4) Choi, S.; Kim, K. W.; Choi, J. S.; Han, S. T.; Park, Y. I.; Lee, S. K.; Kim, J. S.; Chung, M. H. *Planta Med.* **2002**, *68*, 330–335.
(5) Berges, R. R.; Kassen, A.; Senge, T. *Br. J. Urol. Int.* **2000**, *85*, 842–846.
(6) Klippel, K. F.; Hiltl, D. M.; Schipp, B. *Br. J. Urol.* **1997**, *80*, 427.
(7) Berges, R. R.; Windeler, J.; Trampisch, H. J.; Senge, T. H. *Lancet* **1995**, *345*, 1529–1532.
(8) Awad, A. B.; Von Holtz, R. L.; Cone, J. P.; Fink, C. S.; Chen, Y. C. *Anticancer Res.* **1998**, *18*, 471–473.
(9) Awad, A. B.; Chen, Y. C.; Fink, C. S.; Hennessey, T. *Anticancer Res.* **1996**, *16*, 2797–2804.
(10) Lau, V. W. Y.; Journoud, M.; Jones, P. J. H. *J. Clin. Nutr.* **2005**, *81*, 1351–1358.
(11) Park, E. H.; Kahng, J. H.; Lee, S. H.; Shin, K. H. *Fitoterapia* **2001**, *72*, 288–290.
(12) Yoshida, Y.; Niki, E. *J. Nutr. Sci. Vitaminol.* **2003**, *49*, 277–280.
(13) Li, C. R.; Zhou, Z.; Lin, R. X.; Zhu, D.; Sun, Y. N.; Tian, L. L.; Li, L.; Gao, Y.; Wang, S. Q. *J. Cell. Biochem.* **2007**, *102*, 748–58.
(14) Paniagua-Pérez, R.; Madrigal-Bujaidar, E.; Reyes-Cadena, S.; Álvarez-González, I.; Sánchez-Chapul, L.; Pérez-Gallaga, J.; Hernández, N.; Flores-Mondragón, G.; Velasco, O. *Arch. Toxicol.* **2008**, *82*, 615–622.
(15) He, X. M.; Carter, D. C. *Nature* **1992**, *358*, 209–215.
(16) Curry, S.; Mandelkow, H.; Brick, P.; Franks, N. *J. Mol. Biol.* **1998**, *5*, 827–835.
(17) Curry, S.; Brick, P.; Franks, N. P. *Biochem. Biophys. Acta* **1999**, *1441*, 131–140.
(18) Bhattacharya, A. A.; Grnne, T.; Curry, S. *J. Mol. Biol.* **2000**, *303*, 721–732.
(19) Petitpas, I.; Grnne, T.; Bhattacharya, A. A.; Curry, S. *J. Mol. Biol.* **2001**, *314*, 955–960.
(20) Ghuman, J.; Zunszain, P. A.; Petitpas, I.; Bhattacharya, A. A.; Otagiri, M.; Curry, S. *J. Mol. Biol.* **2005**, *353*, 38–52.
(21) Beauchemin, R.; N'soukpoe-Kossi, C. N.; Thomas, T. J.; Thomas, T.; Carpentier, R.; Tajmir-Riahi, H. A. *Biomacromolecules* **2007**, *8*, 3177–3183.
(22) Kanakis, C. D.; Tarantilis, P. A.; Tajmir-Riahi, H. A.; Polissiou, M. G. *J. Agric. Food. Chem.* **2007**, *55*, 970–977.

(23) N'Soukpoe-Kossi, C. N.; Sedaghat-Herati, R.; Ragi, C.; Hotchandani, S.; Tajmir-Riahi, H. A. *Int. J. Biol. Macromol.* **2007**, *40*, 484–490.
(24) Varshney, A.; Sen, P.; Ahmad, E.; Rehan, M.; Subbarao, N.; Khan, R. H. *Chirality.* **2009**, *22*, 77–87.
(25) Shcharbin, D.; Klajnert, B.; Mazhul, V.; Bryszewska, M. *J. Fluoresc.* **2005**, *15*, 21–26.
(26) Charbonneau, D.; Beauregard, M.; Tajmir-Riahi, H. A. *J. Phys. Chem. B* **2009**, *113*, 1777–1784.
(27) Gelamo, E. L.; Silva, C.; Imasato, H.; Tabak, M. *Biochim. Biophys. Acta* **2002**, *1594*, 84–99.
(28) Chuang, V. T. G.; Otagiri, M. *Biochim. Biophys. Acta* **2001**, *1546*, 337–345.
(29) Sugio, S.; Kashima, A.; Mochizuki, S.; Noda, M.; Kobayashi, K. *Protein Eng.* **1999**, *12*, 439–446.
(30) Krishnakumar, S. S.; Panda, D. *J. Biochem.* **2002**, *41*, 7443–7452.
(31) Il'ichev, Y. V.; Perry, J. L.; Simon, J. D. *J. Phys. Chem. B* **2002**, *106*, 452–459.
(32) Subramanyam, R.; Gollapudi, A.; Bonigala, P.; Chinnaboina, M.; Amooru, D. G. *J. Photochem. Photobiol., B* **2008**, *94*, 8–12.
(33) Subramanyam, R.; Goud, M.; Sudhamalla, B.; Reddeem, E.; Gollapudi, A.; Nellaepalli, S.; Yadavalli, V.; Chinnaboina, M.; Amooru, D. G. *J. Photochem. Photobiol., B* **2009**, *95*, 81–88.
(34) Gokara, M.; Sudhamalla, B.; Amooru, D. G.; Subramanyam, R. *PLOS One* **2010**, *5* (1), e8834.
(35) Neelam, S.; Sudhamalla, B.; Gokara, M.; Amooru, D. G.; Subramanyam, R. *J. Phys. Chem. B* **2010**, *114*, 3005–3012.
(36) Lansky, E. P.; Paavilainen, H.M.; Pawlus, A. D.; Newman, R. A. *J. Ethnopharmacol.* **2008**, *119*, 195–213.
(37) Singh, R. K.; Mehta, S.; Jaiswal, D.; Rai, P. K.; Watal, G. *J. Ethnopharmacol.* **2009**, *123*, 110–114.
(38) Kuo, K. H.; Li, Y. C. *J. Chin. Chem. Soc.* **1997**, *44*, 321–325.
(39) Jones, G.; Willett, P.; Glen, R. C. *J. Mol. Biol.* **1995**, *245*, 43–53.
(40) Jones, G.; Willet, P.; Glen, R. C.; Leach, A. R.; Taylor, R. *J. Mol. Biol.* **1997**, *267*, 727–748.
(41) Verdonk, M. L.; Cole, J. C.; Hartshorn, M. J.; Murray, C. W.; Taylor, R. D. *Proteins* **2003**, *52*, 609–623.
(42) Morris, G. M.; Goodsell, D. S.; Halliday, R. S.; Huey, R.; Hart, W. E.; Belew, R. K.; Olson, A. J. *J. Comput. Chem.* **1998**, *19*, 1639–1662.
(43) Berendsen, H. J. C.; Van der Spoel, D.; Van Drunen, R. *Comput. Phys. Commun.* **1995**, *91*, 43–56.
(44) Lindah, E.; Hess, B.; Van der Spoel, D. *J. Mol. Model.* **2001**, *7*, 306–317.
(45) Van Gunsteren, W. F.; Billeter, S. R.; Eising, A. A.; Hünenberger, P. H.; Krüger, P. K. H. C.; Mark, A. E.; Scott, W. R. P.; Tironi, I. G. *Biomolecular Simulation: The GROMOS96 Manual and User Guide*; Vdf Hochschulverlag AG: Zürich, 1996.
(46) Van Gunsteren, W. F.; Daura, X.; Mark, A. E. The GROMOS force field. In *Encyclopedia of Computational Chemistry*; Von Rague Schleyer, P., Ed.; Wiley and Sons: Chichester, UK, 1998; Vol. 2, pp 1211−1216.
(47) Schuttelkopf, A. W.; Van Aalten, D. M. F. *Acta Crystallogr.* **2004**, *60*, 1355–1363.
(48) Berendsen, H. J. C.; Postma, J. P. M.; Van Gunstetren, W. F.; Hermans, J. Interaction models for water in relation to protein hydration. In *Intermolecular Forces*; Pullman, B., Ed.; Reidel: Dordrecht, The Netherlands; 1981, 331−342.
(49) Sulkowska, A. *J. Mol. Struct.* **2002**, *614*, 227–232.
(50) Zsila, F.; Bikadi, Z.; Simonyi, M. *Biochem. Pharmacol.* **2003**, *65*, 447–456.
(51) Dufour, C.; Dangles, O. *Biochim. Biophys. Acta* **2005**, *1721*, 164–173.
(52) Jiang, Y. L. *Bioorg. Med. Chem.* **2008**, *16*, 6406–6414.
(53) Bourassa, P.; Kanakis, C. D.; Tarantilis, P.; Pollissiou, M. G.; Tajmir-Riahi, H. A. *J. Phys. Chem. B* **2010**, *114*, 3348–3354.
(54) Li, D.; Ji, B.; Sun, H. *Spectrochim. Acta A: Mol. Biomol. Spectrosc.* **2009**, *73*, 35–40.
(55) Kanakis, C. D.; Tarantilis, P. A.; Polissiou, M. G.; Diamantoglou, S.; Tajmir-Riahi, A. *J. Mol. Struct.* **2006**, *798*, 69–74.
(56) Beauchemin, R.; N'soukpoe'-Kossi, C. N.; Thomas, T. J.; Thomas, T.; Carpentier, R.; Tajmir-Riahi, H. A. *Biomacromolecules* **2007**, *8*, 3177–3183.
(57) N'soukpoe-Kossi, C. N.; Sedaghat-Herati, R.; Ragi, C.; Hotchandani, S.; Tajmir-Riahi, H. A. *Int. J. Biol. Macromol.* **2007**, *40*, 484–490.
(58) Zunszain, P. A.; Ghuman, J.; McDonagh, A. F.; Curry, S. *J. Mol. Biol.* **2008**, *381*, 394–406.
(59) Kiselev, M. A.; Gryzunov, Y. A.; Dobretsov, G. E.; Komarova, M. N. *Biofizika* **2001**, *46*, 423–427.
(60) Fang, H. W.; Hsieh, M. C.; Huang, H. T.; Tsai, C. Y.; Chang, M. H. *Colloids Surf., B: Biointerfaces* **2009**, *68*, 171–177.
(61) Fujiwara, S; Amisaki, T. *Proteins* **2006**, *64*, 730–739.
(62) Deeb, O.; Rosales-Hernández, M. C.; Gómez-Castro, C.; Garduño-Juárez, R.; Correa-Basurto, J. *Biopolymers* **2010**, *93*, 161–170.

JP102730P